ISSN 1064-2293, Eurasian Soil Science, 2023, Vol. 56, No. 10, pp. 1479–1497. © Pleiades Publishing, Ltd., 2023.
ISSN 1064-2293, Eurasian Soil Science, 2023. © Pleiades Publishing, Ltd., 2023.

MINERALOGY AND MICROMORPHOLOGY OF SOILS

Mineralogical and Micromorphological Properties of Oued Righ Region Soils in the Northern Sahara of Algeria

H. Samia[a, b, *] (ORCID: 0000-0002-5812-4511), B. Hamdi-Aïssa[a], and M. Tewfik[c]

[a] *Univ Kasdi Merbah Ouargla, Fac. Nature and Life Sciences, Earth and Universe, Labo. Biogeochemistry of Desert Areas, Ouargla, 30000 Algeria*

[b] *Scientific and Technical Research Center for Arid Areas (CRSTRA), Biophysical Environment Station, National Road No. 03 Ain Sahara, Nezla, Touggourt, 30240 Algeria*

[c] *Scientific and Technical Research Center for Arid Areas (CRSTRA), Biskra, 7000 Algeria*

**e-mail: helimisamial@yahoo.fr*

Received December 28, 2022; revised April 17, 2023; accepted May 24, 2023

Abstract—Soil resources and their quality in the desert region of Oued Righ, located in northeastern Algerian Sahara, have emerged as unifying concepts to approach the larger issue of sustainability of oasian ecosystems in general, and agriculture in particular. This study aims to characterize and classify using physicochemical, mineralogical and micromorphological analyses, thirteen pedons located in different landscapes positions, including butte, plateau, piedmont, alluvial plain, playa, and claypan, to provide information about the genesis, classification, and properties of the Oued Righ soils. The results showed that the parent materials (calcareous and gypsiferous), as well as the topographic conditions, greatly influence soil development and its distribution in the study area. The soils of the Oued Righ region are generally slightly alkaline and saline, have coarse texture, especially at the soil surface, and are very rich in gypsum accumulations. These soils are classified as Aridisols and Entisols. The clay mineralogy results revealed that detrital input and inheritance are possibly the main sources of palygorskite, kaolinite, smectite-chlorite, and illite. Thin-section observations revealed that calcite coatings on grains and voids, calcite nodules and gypsum macro- and microcrystals were common pedofeatures observed in the studied soils. Hence, the actual hydrological regime in the study area is not compatible with the data obtained; therefore, the majority of pedons should be considered as paleosols.

Keywords: Aridisols, gypsiferous soils, paleoenvironmental conditions, Sahara, pedogenesis, clay mineralogy

DOI: 10.1134/S1064229322602748

INTRODUCTION

Arid regions occupy 26–35% of the Earth's land surface. They are mainly found in Africa, Asia, and Australia. Approximately 43% of the African continent is composed of drylands. Furthermore, hyperarid or desert land compose 38% of these drylands. Half of the African population inhabits these arid regions [48].

Agricultural resources in arid zones are limited in comparison with the population. Continual demands from growing population require the establishment of new irrigated perimeters to maintain the socio-economic balance of these regions. Land reclamation, productivity improvement and soil conservation require even more detailed studies than elsewhere, especially the edaphic factors.

In general, the soils in arid regions pose enormous development problems. They are primarily salty, have calcareous or gypsum crusts, and are susceptible to erosion and secondary salinization [77]. As a result, inadequate soil use and management usually lead to irreversible damage with serious short- and long-term consequences. More than 80% of the Algerian territory is covered by the Sahara Desert. The whole area is occupied by various landscape types with different parent materials. However, pedological studies remain few and very limited [19, 22, 30].

The growing interest in Saharan agriculture in Algeria during the last two decades has introduced a structural transformation in the oasian production system. The Oued Righ region has witnessed a revival, expressed mainly in the extension of irrigated agriculture. Therefore, improved characterization and rational management of natural resources, especially soil and water, has become a primary objective.

The present study concerns the characterization of soils of the upper and middle Oued Righ region, located in the Northeastern Sahara of Algeria. There is limited information on the characteristics of soils in the Oued Righ region, and the existing knowledge is essentially based on the former soil studies providing few details, which limits proper planning for land-use practices [10, 22, 65]. The exception is the study by Boumaraf [11] of the northern edge of Chott Mer-

ouane (Lower Oued Righ) related the spatial evolution of some soils as related to their position on certain geomorphological units.

Soil properties are strongly affected by topography and position along the landscape due to differential erosion, deposition processes, water percolation, and runoff. According to Nettleton [51], the potential use and response of arid soils to management strategies are highly related to the properties imparted to these soils by the accumulation of carbonates, gypsum, and silica. Arid soils inherit many parent material properties because they contain insufficient available moisture, which limits chemical weathering.

The contribution of the clay mineralogy to soil properties depends on the intensity of weathering, which differs from one environment to another. Various studies conducted on the clay minerals in the Algerian Sahara have shown the existence of chlorite, illite, smectite, vermiculite, and palygorskite [11, 15, 19, 30].

The fabric, composition and pedofeatures of gypsic, calcic, or salic horizons are the main indicators of climatic changes [62]. Therefore, in soils of arid and semi-arid environments, micromorphology studies may provide valuable data on soil-forming factors, processes, and climatic changes (paleoclimate) [67]. Various studies have reported high amounts of gypsum in soil with many forms of gypsum accumulation. In the northeastern Algerian Sahara (Low Sahara), Hamdi-Aissa [30] reported lenticular, tabular, and hexagonal gypsum crystals being related to soil moisture content, landscape position, and soil development stage. The source of gypsum crystals was determined by using the shape, size, and position of the crystals within the soil matrix. The presence and accumulation of calcium carbonate in arid soils have been the subject of intensive research because its presence and morphology are good indicators of pedogenic environments, pedogenic processes, and soil moisture regimes. According to Chadwick et al. [14], the main factors determining carbonate morphology were precipitation rate, soil solution ionic strength, and crystal surface interactions with organic and inorganic matter.

Oued Righ is an ideal region for studying the relationship between diverse topography, soil types, and geological formations. Limited data are available to thoroughly describe soils and pedogenesis of this area. Therefore, the objectives of this work were as follows:

(1) To characterize the physicochemical, mineralogical, and micromorphological attributes of thirteen representative soil pedons located on different landforms.

(2) To determine the soil genesis and classification using Soil Taxonomy system.

(3) To provide detailed information for different agricultural and non-agricultural uses.

MATERIALS AND METHODS

Study site. The Oued Righ (Wadi-R'hir) region, located in the northeastern Algerian Sahara (Fig. 1), is part of the entire Lower Sahara basin [8]. This region is in the form of a large gutter 15–30 km wide, extending to more than 150 km in length. The study area lies between 32°45′–34°30′ N latitude and 5°45′–6°15′ E longitude. The altitude gradually decreases from +100 m in the south to –27 m in the north (in the middle of Chott Merouane).

The study area is characterized by a hyperarid climate [76]. Rare and irregular precipitation (60 mm average in the 2007–2016 period) and high temperatures with intense daily and seasonal variations are observed. The mean annual temperature is 22.5°C [54]. The air has a low relative humidity, wind gusts are frequent and violent, and sunshine is constant and very intense.

Geology and geomorphology. The study area is located in the Lower Sahara, which extends between the southern Occidental Atlas and the first foothills of the Aures Mountains in the north [33]. The geological formations are mostly of Quaternary age, resulting from continental erosion of Mio-Pliocene deposits.

Oued Righ is a vast depression elongated on a South-North axis. It joins the Wadi Djedi gutter and is flagged by fossil wadis, with the Mya and Igharghar valleys to the South and Oued Righ to the north [8]. The large Oued Righ gutter represents the downstream part, which is more or less blocked by sandy veneers and shifting dunes. Four distinct levels appear in the Oued Righ region:

• the upper level is represented either by gypsum crust glacis (Stil Plateau) or by residual surfaces appearing in outcrops with more or less uneven relief;

• the intermediate level generally characterizes ancient quaternary glacis, and soils are sandy and rich in gypsum;

• the pre-chotts appear at a level below and represent flat surfaces with a low slope;

• the chotts represent the lowest areas of the valley with excessively saline soils.

Soil sampling and analysis. Six dominant physiographic units were identified: plateau, butte, piedmont plain, alluvial plain, playa, and claypan, which were defined in the study area using a digital elevation model (DEM), Google Earth and topographical maps, together with detailed fieldwork. Thirteen representative soil pedons were studied to characterize the soil cover organization of different geomorphological units, and the soils were described and classified according to the Soil Survey Staff (2014) [66] and the World Reference Base (WRB) (2022) [74]. Forty-six soil samples were taken from all horizons for laboratory analyses, and disturbed samples were used for physical, chemical and mineralogical analyses. Other undisturbed samples were chosen for micromorphological observations.

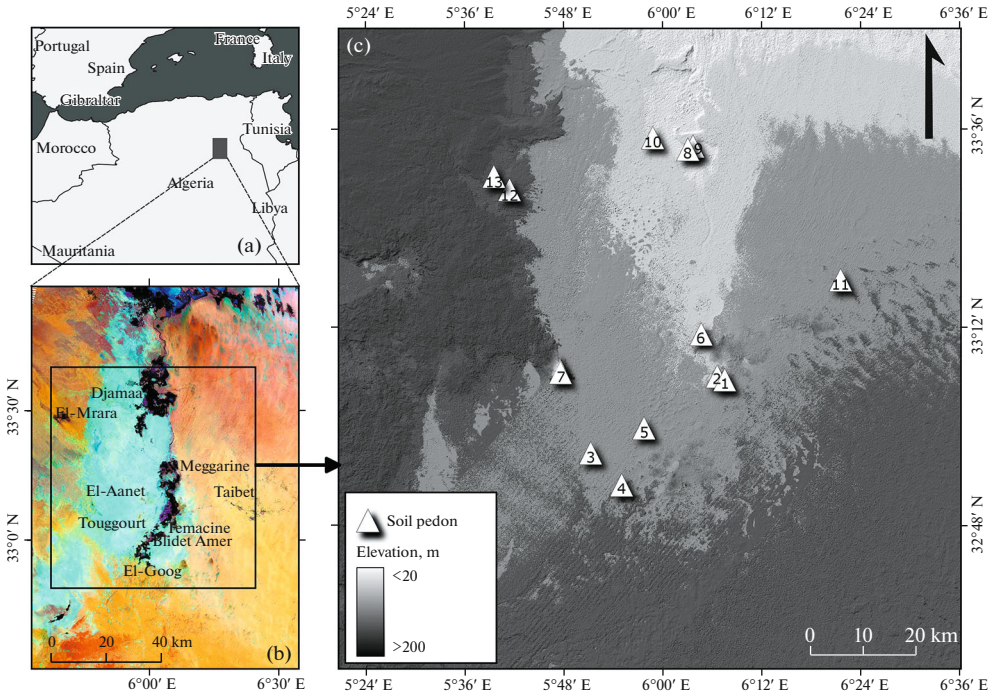

Fig. 1. The geographic location of the study area (a), Landsat 5 TM image (false-color composite of bands 7, 4, and 1 (b), spatial distribution of soil pedons draped over a Digital Terrain Model (DTM, resolution of 30 m) (c).

Physical and chemical analyses. To determine physical and chemical soil properties, disturbed soil samples were air-dried, ground, and passed through a 2-mm sieve to obtain the fine earth fraction. Soil texture was assessed by determining the grain size distribution, sand fractions were separated by wet sieving, oven-dried and then weighed, silt and clay were determined by pipette with soil H_2O_2 pretreatment to remove organic matter, and calcium carbonate was determined by HCl. Total calcium carbonate was measured by the volumetric method of the Bernard calcimeter [6]. The gypsum content was measured with the amended $BaSO_4$ method [18]. Soil electrical conductivity (EC) and pH were measured in solution (1 : 5 soil/water) [6, 66]. Finally, the soil organic carbon (OC) content was determined with the dichromate oxidation method of Anne [3].

Mineralogical analysis. The mineralogical analysis was conducted by XRD equipment at the Central Laboratory of INRAE (Centre de Versailles-Grignon, France). Samples from pedons 1, 2, 3, 4, 5, 7, and 10 were prepared for the determination of clay fractions according to the method described by Robert and Tessier [60]. The method started by destroying organic matter and decarbonating soil samples. Then, different mechanical and chemical treatments were used to disperse the clay fraction and obtain magnesian clay by the addition of $MgCl_2$.

The measurements were carried out according to the oriented clay deposits method. The slides are scanned using a Bruker D8 advance diffractometer with a copper anode and coupled graphite crystal monochromator, operating at 45 kV and 30 mA, at a speed of 0.01/0.5 s at 2–35° 2θ. Clay mounts were prepared and scanned using Ca saturation, solvation with ethylene glycol and heating to 110°C for the pedon 5 sample and to 200, 350 and 550°C for the other samples. X'Pert HighScore Plus 3.0 software was used for the identification and quantification phase of the samples studied.

Micromorphological study. Twelve samples were impregnated with polyester resin; thin sections were prepared of 13.5/6.5 cm in size, oriented vertically, according to the protocol proposed by Guilloré [26]. The thin sections were prepared in the micromorphological laboratory of the National Agronomic Institute Paris-Grignon and analyzed under an OPTIKA B-600POL Trinocular Polarizing Microscope. Thin sections were described according to Bullock et al. [13], Fedoroff and Courty [24], and Verrecchia and Trombino [71].

RESULTS AND DISCUSSION

Morphological characteristics. Table 1 shows the main morphological characteristics of different soil layers in pedons. The soils have Munsell colors ranging from 10YR to 10GY. The soils with calcium carbonates, gypsum, or other more soluble salts have light colors, and the poorly drained and heavier soils have darker colors.

Table 1. Morphological description, physicochemical properties of the studied pedons

Pedon N	Physiography				Coordinates and elevation (m)					Classification				
										ST (2014)			WRB (2022)	
Hz	depth, cm	color moist	text	strut	cons	special features	pH	$EC_{1:5}$	sand	silt	clay	CCE	gypsum	OC
								dS/m	%					
1	Tabular butte Witness (Mound Witness)				33°6′4.17″ N, 6°6′35.79″ E, *h* 103 m					Typic Calcigypsids			Calcic Gypsisols	
Ay	0–28	7.5YR 4/7	S	Sg	fr		7.6	9.59	86	12.8	1.2	13	51.75	0.58
B ky	28–45	7.5YR 6/6	LS	2M	fr		8.5	9.78	80	15.9	4.1	21	67.34	0.47
Bkyc	45–60	7.5YR 7/4	LS	1m Sg + M	fr	Nodules + rhyzoliths and gypsum rosette crystal	7.7	10.76	82.2	16.8	1	26	53.11	0.64
Cky1	60–190	7.5YR 5/6	LS	1m Sbk	fr	Limestone powdery pockets	7.6	7.79	80.3	15.6	4	15	52.66	0.93
C 2	>190	7.5YR 5/6	SL	2c Sbk	st		7.6	8.71	78.4	7.8	13.8	19	67.5	0.76
Ay	0–28	7.5YR 4/7	S	Sg	fr		7.6	9.59	86	12.8	1.2	13	51.75	0.58
2	Piedmonts				33° 6′ 3,7″ N, 6°6′ 42,10″ E, *h* 100 m					Typic Argigypsids			Luvic Calcic Gypsisols	
Aky	0–40	7.5YR 5/3	SCL	2m Sbk	fr	Patche of gypsum crust on soil surface	7.6	8.5	13.5	50.8	35.7	22	66.79	0.64
Bt	40–58	7.5YR 5/3	C	3c Sbk	st	Gypsum rock fragments	8.15	8.7	17.2	38	44.8	27	67.37	0.47
C	58–67	2.5Y	–	3c Pl	st	Fibrous gypsum veins	–	–	–	–	–	–	–	–
3	Piedmonts				32° 6′53,41″ N, 5°54′58″ E, *h* 127 m					Typic Calcigypsids			Petric Calcic Gypsisols	
Ay	0–135	10YR 6/6	S	2cM	st	Gypsum crust	7.5	5	89.13	7.8	3.07	25	67	0.64
Bky	135–155	7.5YR 5/8	LS	2m Sg + M	fr	Rhyzoliths + gypsum rose crystal	8.2	4.8	85.6	10.3	4.1	27	56.17	0.52
C	>155	5YR 5/6	S	1m Sg	vfr		8.1	4.4	90.5	7.5	2	30	44.5	0.7
4	Alluvial Plain (Clay quarry)				32°52′55,42″ N, 5°55′0,83″ E, *h* 120 m					Lithic Argigypsids			Leptic Gypsiric Fluvisols	
Ay	0–35	7.5YR 5/8	CL	1f Sbk	fr		7.09	5.26	43.88	21.3	34.82	0.78	59.79	0.31
Bty	35–50	7.5YR 5/6	C	1f Pl	fr		7.24	8.42	38.4	19.5	42.15	1.79	35.25	0.41
1Cyz	50–70	7.5YR 6/4	CL	1m M	st	Thin gypsum veins	7.87	5.87	44.74	25.5	30.76	0.78	67.03	0.20
2Cy	70–74	7.5YR 5/6	SCL	2m Pl	st		7.5	4.97	58.69	16.2	25.12	1.12	65.5	0.50
1Cyc2	74–86	7.5YR 6/4	LS	1m M	st	Nodular gypsum layer	7.3	2.86	82.92	6.28	10.8	0.67	61.39	0
2C2	86–100	7.5YR 5/6	CL	2m Pl	st		8.15	7.82	42.2	20	37.82	1.14	15.34	0.80

Table 1. (Contd.)

Pedon N	Physiography				Coordinates and elevation (m)					Classification				
										ST (2014)		WRB (2022)		
Hz	depth, cm	color moist	text	strut	cons	special features	pH	$EC_{1:5}$	sand	silt	clay	CCE	gypsum	OC
								dS/m		%				
R	>100	7.5YR 6/4	SCL	1m M	st		7.2	6.12	55.33	16.6	28.1	0.56	75.12	0
5	Alluvial Plain				32°59′49,34″ N, 5°57′43″ E, *h* 92 m					Typic Calcigypsids		Calcic Gypsisols		
Aky	0–49	7.5YR 5/6	LS	Sg+M	fr	Gypsum crust	8.17	4.64	80	16.7	3.3	25	52.38	0.87
Ckyc1	49–115	7.5YR 5/6	SL	Sg+M	fr	Gypsum rosette crystal + limestone nodules	7.5	2.6	74.4	15.5	10.1	30	64.3	1.1
Cky2	115–190	5YR 7/3	SL	2m Sbk	st	Limestone powdery	7.55	3.62	76.1	10.1	13.8	26	62.8	0.58
R	>190	7.5YR 5/3	SL	1m M	fr		8.25	2.5	78.1	12.4	11.5	25	50.47	0.7
6	Plain surface				33°11′11″ N, 6°4′39,17″ E, *h* 66 m					Petronodic Calcigypsids		Yermic calcic Gypsisols		
Aky	0–60	10YR 6/4	S	Sg	fr		7.8	4.7	89	8.5	2.5	10	58.1	0.52
Ckyc1	60–130	7.5YR 5/6	LS	Sg+M	fr	Gypsum rose crystal + gypsum rock fragments	7.8	3.1	85.8	9.1	5.1	13	47.37	0.85
Cky2	130–163	10YR 7/6	LS	Sg+M	fr		7.5	3.05	85	11.5	3.5	9	41.1	0.29
R	>163	2.5YR 7/6	S	Sg	fr		7.6	4.15	90.5	8	2.5	15	33.07	0.29
7	Low plateau (Tabular Butte)				33°7′31,40″ N, 5°47′12,88″ E, *h* 113 m					Typic Petrogypsids		Yermic Epipetric Gypsisols		
Ayym	0–54	7.5YR 8/2	S	3c M	st	Gypsum tabular crust	7.61	7.61	87.15	10.2	2.7	4.80	68.5	0.35
Cy1	54–103	7.5YR 8/6	LS	2f M	fr	More than 45% gypsum nodules and Concretions.	7.85	7.85	78	16.1	5.9	10.1	50.17	0.23
C2	103–215	7.5YR 7/6	SL	2f Sbk	fr		8.16	8.16	65	22.7	12.26	11.1	43.1	0.47
8	Main Wadi channel				33°33′54.9″ N, 6°3′39″ E, *h* 27 m					Typic Haplogypsids		Gypsic Gleyic Solonchaks		
Ap	0–36	7.5YR 7/6	SL	Sg	fr	Salt efflorescence on soil surface	7.35	11.17	68.3	19.7	12	2.81	10.4	1.10
Bg	36–62	2.5Y 4/1	LS	Sg	fr	GleyGley with over 40% abundance	7.04	9.77	83.7	11.4	4.9	2.19	8.2	1.50
9	Playa				33°33′59.8″ N, 6°04′04″ E, *h* 23 m					Gypsic Aquisalids		Gypsic hayoersalic Solonchaks		
Az	0–15	7.5YR 6/4	LS	Sg	fr	White salt crust on soil surface	7.06	30.44	83.8	10.1	6	1.5	6.64	0.92

Table 1. (Contd.)

Pedon N	Physiography				Coordinates and elevation (m)					Classification				
										ST (2014)			WRB (2022)	
Hz	depth, cm	color moist	text	strut	cons	special features	pH	$EC_{1:5}$ dS/m	sand %	silt	clay	CCE	gypsum	OC
Cy	15–75	7.5YR 6/6	SL	Sg	fr	Water table level at75 cm	7.15	25.64	72.5	17.4	10.1	0.7	13.5	0.96
10	Piedmont				33°34′57.5″ N, 05°58′46.9″ E, *h* 44 m					Typic Petrogypsids			Gypsic Duric Solonchaks	
Ayym	0–67	7.5YR 5/6	LS	3c M	st	Gypsum crust	7.1	11.8	85.8	9.75	4.45	0.3	40.38	0.87
Cy1	67–131	7.5YR 6/6	LS	1m M	st	Gypsum rose crystal + Rhizoliths	7.87	23.76	81.5	11.5	7	0.5	29.19	1.05
C2	>131	7.5YR 6/6	LS	Sg+M	fr		7.36	21.47	86.9	8.82	4.28	1	15.36	1.05
11	Dune area				33°17′44,52″ N, 6°21′32″ E, *h* 92 m					Typic Torripsamments			Skelitic Arenosols	
A	0–23	7.5YR 5/6	LS	Sg	vfr		8.06	2.06	78.8	16.4	4.8	4.5	9.1	0.09
C	23–110	7.5YR 5/8	SL	Sg	vfr		8.15	1.93	73.4	20.3	6.3	2.88	6.22	0.06
12	Claypan fond (Daya)				33°28'39.4″ N, 5°41'26″ E, *h* 106 m					Anthropic Torrifluvents			Calcaric Skeletic Fluvisols	
Ap	0–30	7YR 5/8	LS	Sg	vfr		8.1	0.6	80.22	15.3	4.5	7.3	10.04	2.15
C1	30–45	5YR 6/6	LS	1f pl	fr		8.03	0.7	81.6	12.6	5.8	11.8	9.25	1.20
2C	45–83	7YR 5/6	S	Sg	vfr		8.2	0.68	95.7	4.3	0	4.5	4.13	0.77
1C2	83–93	5YR 6/6	LS	2m pl	fr		8.11	0.56	83.74	11.9	4.4	10.2	7.8	1.01
3C	>93	5YR 4/6	S	Sg+M	fr		7.98	0.79	89.69	7.11	3.2	15	6.56	0.4
13	Claypan border				33°30′16.27″ N, 5°39″31.72″ E, *h* 119 m					Typic Torriorthents			Calcaric Yermic Fluvisols	
Ay	0–31	7.5YR 6/6	S	Sg	fr	Medium gravel 30% sub angular	8.45	2.98	93.07	6.18	0.75	4.5	8.22	0.34
Ckc1	31–62	5YR 6/6	LS	Sg	fr	Rock fragments more than 40% sub rounded and rounded + limenstone barbs	8.29	3.19	86	5.7	8.3	22.5	5.10	0.28
C2	>62	7.5YR 5/8	S	Sg	fr		8.3	3.73	88.45	8.05	3.5	15.2	3.85	0.29

Abbreviations. Hz—Horizon. Text—Texture. Stru—Structure: 1—weak; 2—moderate; 3—strong; Sg—single grain; M—massive; Sbk—subangular blocky; vf—very fine; f—fine; m—medium; c—coarse. Cons—Consistance: (Dry); vfr —very friable; fr—friable; st—steady. Boun—Boundary: a—abrupt; c—clear; g—gradual; d—diffuse; s—smooth; w—wavy; i—irregular, EC—Electrical Conductivity. OC—Organic Carbon. CCE—Calcium Carbonate Equivalent.

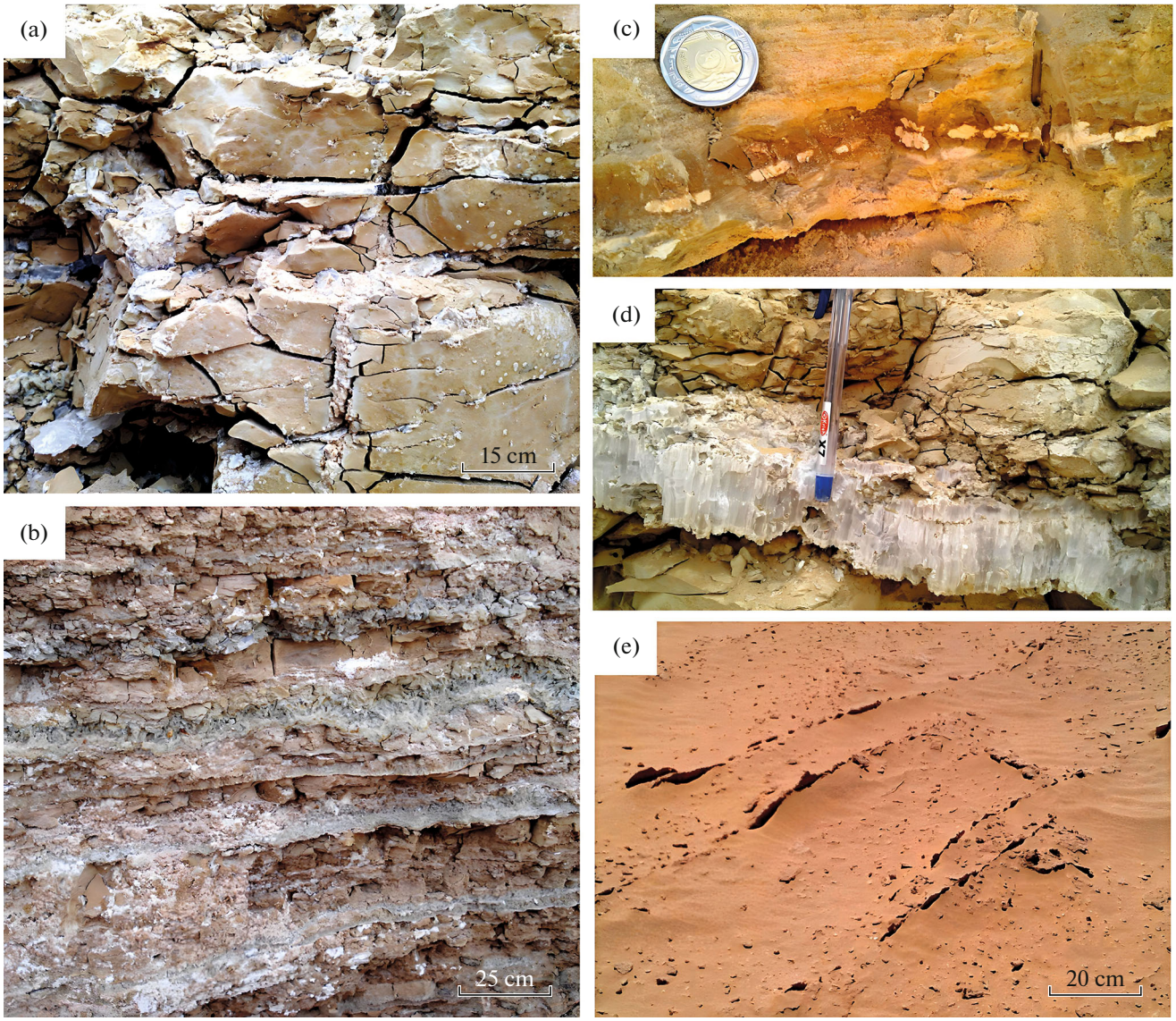

Fig. 2. Veins gypsum, (a) high-density and well-connected joint pattern in miocene marly clays layer filled with fibers gypsum (pedon 2); (b) primary gypsum; gypsum veins interbedded with clay units as thin layers (2 to 15 cm thickness) in djamaa area; (c) white nodular gypsum in lamina layer of silt and clay (pedon 4), will be connected to form horizontal gypsum veins; (d) satin spar veins formed sub parallel with bedding, vein thickness is 7 cm (pedon 2); (e) field view of orthogonal gypsum vein arrays in El-Goug area.

The main morphological characteristics of the studied pedons were gypsic, calcic, salt, and textural features. Pedon 1, located on small mounds, showed gypsum and clay surmounted at the base by approximately 2 m of alternations of quartz sand and gypsum accumulations. Of these formations, only one, composed of sand in subhorizontal beds, 130 cm thick could be of fluvial origin [8]. It lies just below the yellow quartz sandstones carved into the yardangs by the sand transported by the west winds, which may contain clay of neolithic origin. The soil of the alluvial plain (pedons 4 and 5) was composed of formations attributed to the Mio-Pliocene at heights of several tens of meters. Clay and silt, often gypsum-containig, in subhorizontal beds derive of the depositional regime of fluvial systems.

The presence of the gypsic horizon was common in the studied pedons. These micro- and macroscopic gypsum accumulations (powdery, lenticular, sand roses, rhyzoliths, fibrous veins and gypsum crust) (Table 1, Fig. 2) were due to the precipitation of gypsum from the salts contained in the aquifer and runoff [20]. Therefore, gypsum was an important constituent of soil material that contributed to forming soil physical and chemical properties.

Gypsum crusts were omnipresent in Oued Righ region. They could be easily spotted, especially given their significant thickness and whitish color, which generally result from a postdeposition alteration [16]. Thus, the transport and postdeposition redistribution of gypsum sediments occur where wind and water play a very important role. The photointerpretation of TM data (Fig. 1a) shows the large area occupied by the saline gypsic soil surface with important spectral responses of this surface aspect (white soils) cyan-colored area. Hamdi Aissa and Girard [29] reported similar results in gypsic-saline soils in the Ouargla region (Northern Algerian Sahara).

Several researchers have discussed the origin of gypsum crusts [35, 58, 73, 75], and different hypotheses have been proposed to explain their formation. The studied gypsum crusts (pedons 1, 3, 5, 7 and 10) were residual of those described by Watson [73] as surface crusts, originating from degradation of subsurface accumulations and meteoric water dissolution of gypsum crystals, followed by soil conservation, until subsequent evaporation precipitates the soluble salts. However, Dutil [22] attributed the origin of these crusts to a higher level of groundwater. According to Pouget [58], since the beginning of the Quaternary, the static levels of the large artesian basins have dropped by several meters; it is not surprising to find ancient gypsum formations of the water table in places now topographically elevated. Furthermore, gypsum is a very mobile compound in the Lower Sahara landscape despite its moderate water solubility; such displacements imply very different moisture conditions as compared to the present-day ones [22].

The different types of gypsum crystals are undoubtedly related to specific environmental and pedogenetic factors, such as parent material, geomorphological position, climate, and the influence of groundwater [30]. The high content of gypsum found in Oued Right soils seems to be due to the mineralogical composition of the parent material (i.e., evaporitic sediments), but their distribution in pedons depends on groundwater movements.

Calcic features were observed in the study area as powdery pockets, nodules, or calcite coating in Bk or Ck horizons that have formed in alluvial plain (pedon 5), butte (pedon 1), piedmonts (pedon 2 and 3), and claypan (pedon 12 and 13), indicating that calcite is pedogenic. The formation of the calcic horizon between gypsic horizons as a particular combination is proof of polyphase soil genesis. The discontinuity observed in those pedons is another piece of evidence for soil climatic change over time.

In the playa (pedon 10), the influence of the water table is manifested by the extreme salinity of the surface horizon. There is a continuous fragile salt crust characterized by a wavy microtopography with a thickness of 0.5 to 1.2 cm. The salt crust was lying on loamy sand to sandy loam material; the color varied from 7.5 YR6/4 (light brown) to 7.5 YR6/6 (reddish yellow). Pedon 9 was characterized by a saline horizon on the soil surface with whitish efflorescence and a gley horizon with greenish gray color (10GY 5/1) in deeper soil horizons. This problem is explained by the rising of the groundwater table owing to excessive irrigation created by the use of a traditional irrigation system. It comprised border irrigation with an uncontrolled watering duration and interval, an inoperative drainage system and the proximity of this palm grove to the playa. Waterlogging of Oued Righ soils of finer texture is an ancient phenomenon that caused the appearance of hydromorphic characters (gley and pseudogley).

Soil located in the main wadi channel of Oued Righ and the El Mrara Claypan (pedons 4 and 12) have well-stratified layers, characterized by contrasting colors (from 7.5 to 5 YR), structure (single-grain/platy), and platy/massive one. The textural discontinuity mentioned in these pedons indicates that in sedimentary systems characterized by the interaction between alluvial and aeolian processes, aeolian–alluvial interaction is the geomorphic–sedimentary expression of the coexistence and overlapping of alluvial and aeolian environments.

The interactions between alluvial-colluvial and aeolian processes have important implications for the geomorphology of the landscape in arid regions; this is exceptional for alluvial soil formation in arid environments [17, 19]. This idea is confirmed by the study of Sogreah [65], which defines the origin of the soil of the Oued Righ valley as mixed alluvial, colluvial, and aeolian phenomena. The first two are derived from erosion of the encrusted level from the ancient Quaternary and/or Mio-Pliocene. Successive phases of water erosion and filling of the valley bottom are responsible for the textural heterogeneity found in the deep horizons, in contrast to the upper horizons, which have an aeolian origin.

Quartz grain morphology (Fig. 3) and micro-textures on the surface allow the interpretation of sedimentary environments and potential transport mechanisms that are recorded on the grains [72]. The results of stereoscopic observations of quartz grains showed the presence of various shapes with irregular morphologies. There was a mixture of round mat grains characteristic of wind action, angular-shiny grains that result from sandstone disaggregation, and blunt and picketed grains. The omnipresence of shiny blunting grains highlights the influence of water transport precisely in deep soil horizons (Fig. 3b).

Sand grain morphology of the surface horizon (aeolian veil) for most pedons in the study region revealed many traces of shock and dissolution on their surface and that they are agglutinated by gypsum, with a strong presence of gypsum associated with the sand grains (Fig. 3a). The analysis of these samples by X-ray diffraction (XRD) confirmed the dominance of gypsum (Fig. 4).

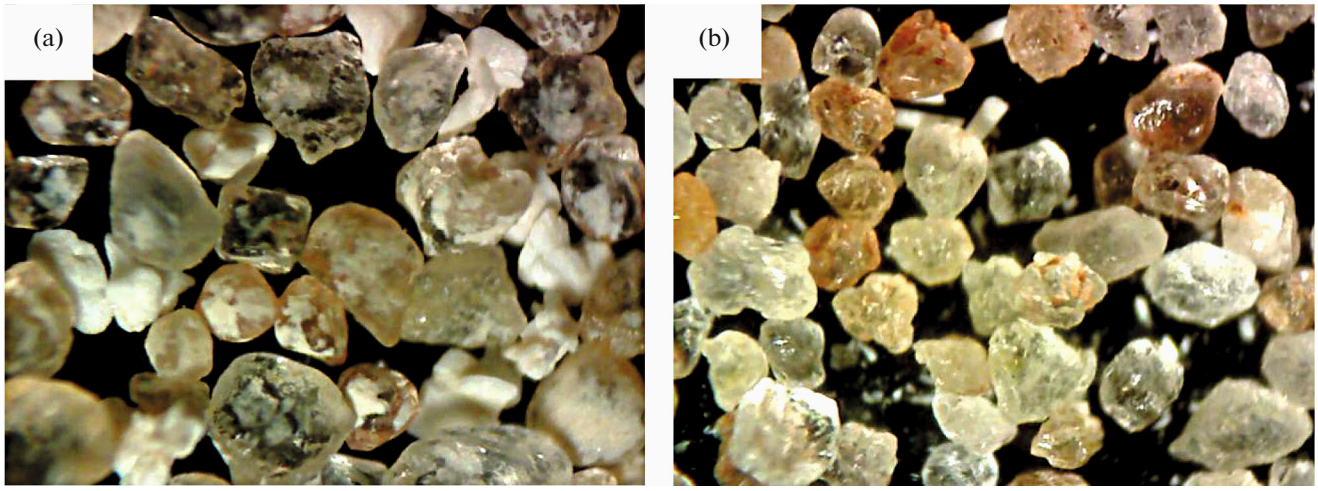

Fig. 3. Quartz grains morphoscopy (×40): (a) sand fractions (500–2000 μm), quartz grains agglutinated by gypsum with strong presence of gypsum fraction in surface horizon (Ay) of pedon 4; (b) sand fraction (2–500 μm), mixture of sub–rounded mats quartz grains, sub–angular shiny grains with presence of a red coating on a few grains (4/2C2).

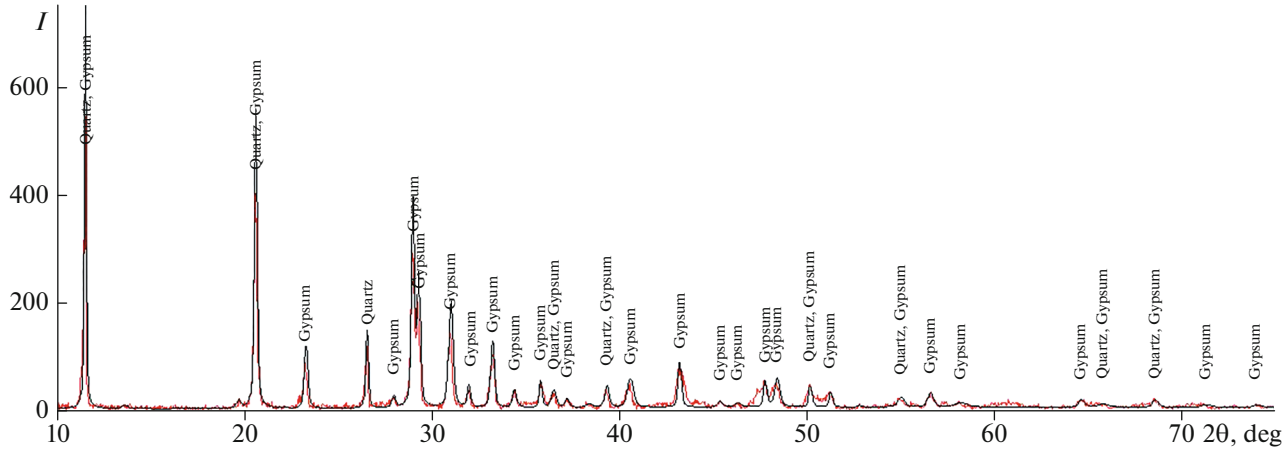

Fig. 4. Representative XRD pattern of the sand fractions (500–2000 μm) of the soil surface (Ay horizon of pedon 4).

Physicochemical characteristics and classification. Soils are generally undeveloped or weakly developed due to the presence at varying depths of gypsic and/or petro-gypsic horizons and conglomerate blocks. The horizons below these crusts undergo compaction as consequence of mechanical pressure exerted on the quartz material by the gypsum. Using the field and laboratory data, the representative soils were classified to the subgroup level of the Soil Taxonomy [66]. The majority of soils were classified as Aridisols (10 pedons) and Entisols (3 pedons). Six major types of gypsic soils were found: Typic Calcigypsids, Typic Argigypsids, Lithic Argigypsids, Petronodic Calcigypsids, Typic Haplogypsids, and Typic Petrogypsids. All of these types were distributed in areas with arid soil moisture regime.

Physicochemical data on the 46 soil samples showed a non-significant variation in pH values among all the soil horizons. It varied from 7.04 to 8.5, and most soil horizons have an alkaline pH; those values are within the normal range because the soils developed on carbonatic and gypsic bedrocks.

EC varied from 0.56 to 25.44 dS/m, indicating a range from nonsaline to excessively saline soils [6]. High EC values were found in the soil horizon located in the salty depression (pedons 9 and 10), where the influence of the water table is decisive. The salinity of the soils of the upper Oued Righ was significantly lower than that of the salic and gypsy-salic soil landscapes further downstream. Irrigated soil (pedon 8) in the Oued Righ valley is vulnerable to hydromorphism and salinization. The most important factors affecting

soil salinity are the climatic characteristics, hydropedological setting, irrigation with poor quality groundwater (salinity greater than 3 g/L) [43], poor drainage system, and land-use patterns.

Soil samples of the studied pedons were classified as loamy sand (LS), sand (S), sandy loam (SL), sandy clay loam (SCL), clay loam (CL), and clay (C), according to the textural soil classification system. The average values for clay, silt, and sand-size fractions were 10.81, 14.35, and 75%, respectively. Therefore, sand is the most abundant fraction. The calcium carbonate equivalent (CCE) and gypsum percentages varied from less than 0.3 to 30% and from 3.85 to 75.12%, respectively. The calcium carbonate content decreases with depth in most pedons in the areas of El-Goug, El-Aanet, and Meggarine, although the opposite trend was expected under arid conditions.

The content and distribution of gypsum within the pedons were affected by the chemical balance with other soluble components, especially $CaCO_3$ and soluble salts [32]. The low total calcium carbonate values compared to gypsum values obtained were due to mechanical disintegration caused by gypsum crystallization pressure, as demonstrated by Richard and Donald [59]. A positive correlation existed in some horizons between the presence of gypsum in powder form and the value of calcium carbonate [12]. Hamdi Aissa [30] noted that the gypsum content of gypsum pedological volume was not an essential factor. There was, in fact, no relationship between gypsum content and volume induration state. We found the same result in this study; a volume with low gypsum content can be indurated (petrogypsic). Conversely, encrusts even with very high gypsum content can be friable or powdery (gypsic).

We found a spatial variation in OC content that was directly related to vegetation cover. The organic carbon content of the studied soils ranges from 0 to 2.15%. Although OC is generally low in such arid environments, the maximum value observed is also found in agricultural land.

The majority of soils in the Oued Righ region were developed on sandy and gypsum formations of the Mio-Pliocene and ancient Quaternary. They were morphologically very similar to each other. This similarity of materials of different ages is probably related to the fact that the sediments of the ancient Quaternary are the result of the erosion of Mio-Pliocene formations, clearly distinguished at their base by gypsy-clay intercalations extending from the south of the Oued Righ valley at El Goug (pedon 4) to the low level of the northern Oued Righ at Djamaa (pedon 10). In some places, these formations have laminated gypsum crusts, which reflects the fluvio-lacustrine origin of these formations due to incision of valleys from the Villafranchian age.

Clay mineralogy. The dominant clay minerals in pedons were palygorskite, illite, kaolinite, and chlorite-smectite (Table 2, Fig. 5). Among the phyllosilicates, there was a dominance of the peaks at approximately 7.14 and 3.57 Å. They disappeared after heating to 550°C, which is generally attributed to kaolinite. There was also palygorskite indicated by the peaks at 6.4 Å and 10.4 Å. Peaks at approximately 10 and 5 Å were indicative of small amounts of micas and/or illites, which did not change positions or intensities after any diagnostic treatments [36]. Gradual heating of Ca-saturated samples from 110 to 300°C reversibly dehydrated (closed) the 2 : 1 minerals, which were identified as vermiculite and smectite.

The low-intensity peak at approximately 3.2 Å was attributed to feldspar (Fig. 5). The peaks at approximately 4.25, 3.34 and 2.24 Å represent quartz; the peak at 14.4 Å in the diffractogram of the sample saturated with Ca seems to be smectite-chlorite.

Kaolinite, illite, chlorite-smectite and palygorskite occurred in major soil horizons, demonstrating the high mineralogical uniformity of those soils. These clay minerals are characteristic of soils in arid and semi-arid environments. Similar results were found by other researchers [1, 61, 70] and were reported in Algerian Sahara soils [11, 19, 30].

The occurrence of clay minerals in soils is due to one of the following major processes: (1) inheritance from parent materials, (2) transformation of other clay minerals, and (3) neoformation from the soil solution [44].

Table 2 Relative mineral components of selected clay fraction (<2 μm) as determined by X-Ray

Pedon N/Hz	*Chlorite*	Smectite	Palygorskite	Kaolinite	Ill-Mic	Chl-Sme	Illite
1/C2	–	+	+++	+	–	–	+
2/Btk	–	–	++	+	+	+++	–
3/Bky	–	–	++	++	+	++	–
5/Cky1	–	–	+++	+	+	++	–
6/Cky1	+	–	++	+	++	–	+
7/C2	+	+	+++	++	–	–	+
13/Ckc1	–	–	+++	++	+	+	+

Note: (–) not detected, (+) <25%, (++) 25 to 50%, (+++) >50%.

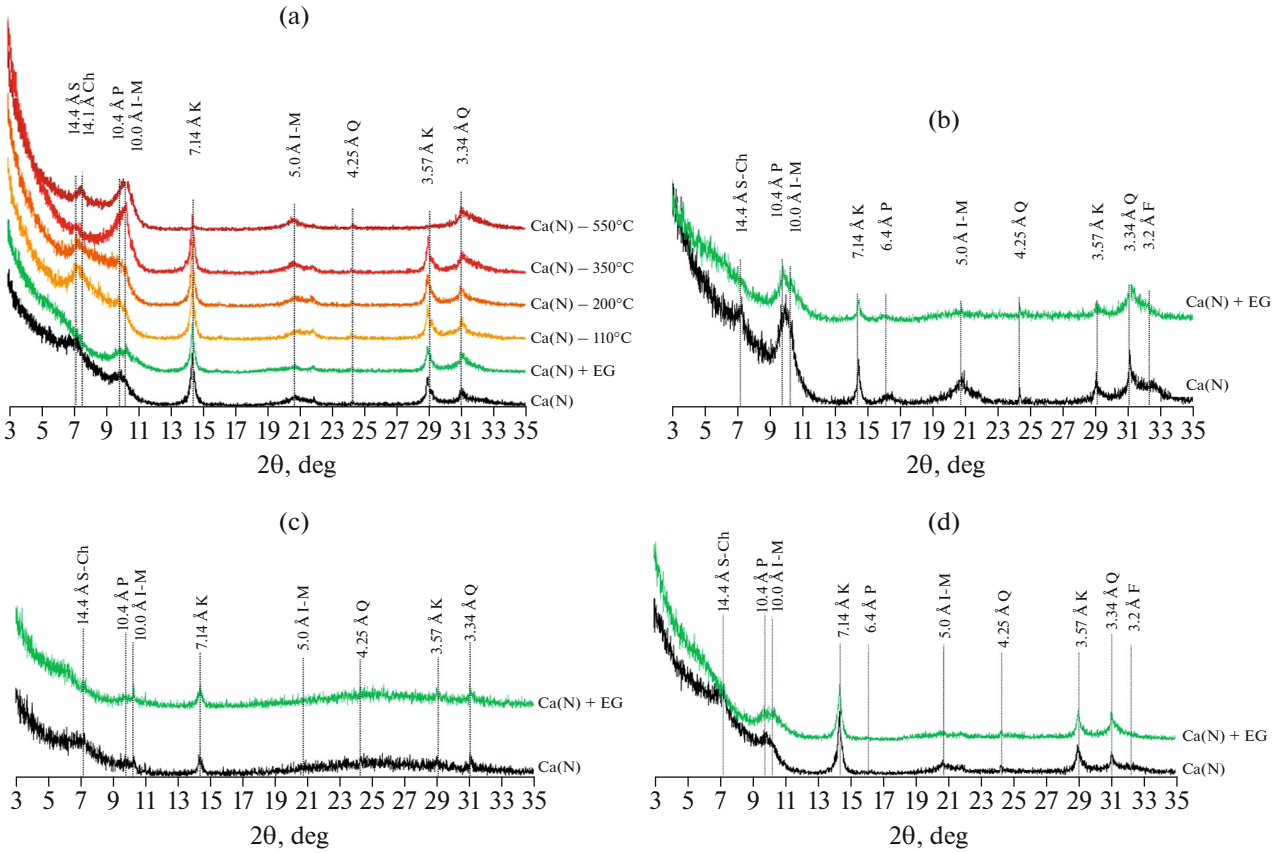

Fig. 5. Representative XRD patterns of total clay fraction (<2 μm) of the pedons from upper Oued Righ: 5/Ckyc1 (a); 2/Btk (b); 3/Bky (c); 13/Ckc1 (d). Smectite (S), Chlorite (Ch), Palygorskite (P), Mica (M), Kaolinite (K), Quartz (Q), Illite (I), and Feldspar (F). Numbers above the peaks correspond to the d spacing in Å. CoKα radiation. Treatments: Ca (N) clay samples saturated with Ca^{2+}; Ca (N) + EG Ca–saturated + Glycerol solvated; Ca (N) – 110 Ca saturated and heated to 110°C; Ca (N) – 200 Ca-saturated and heated to 200°C; Ca (N) – 350 Ca-saturated and heated to 350°C and Ca (N) – 550 Ca-saturated and heated to 550°C.

The presence of moderate to high contents of illite and chlorite in the soils could be related to inheritance from parent rocks [49]. The ideal conditions for chlorite formation in soils are high leaching, low pH, and removal of interlayer hydroxides [55]. The arid moisture regime of the study area is not favorable for the pedogenic formation of chlorite. Therefore, the chlorite of the studied soils is supposed to be inherited from the sediment.

Halitim [27] found that the amount of illite was inversely proportional to the limestone content. However, there is some indication that mica may be formed pedogenically in arid soils as well, but only under special conditions, mainly through K fixation of preexisting smectite [61]. Illite is considered a stable clay mineral in the aridic pedoenvironment. However, Singer [63] noted that the accumulation and distribution of illite in aridic soils could partly be explained by the illitization process; which has taken place (number of deposition deflation/wetting–drying cycles).

Kaolinite was present in almost all analyzed samples, with a strong presence in gypsum and gypsy-salic soils. It is well known that kaolinite forms mainly from feldspars and mica alteration under conditions of low aK+/aH ratios. This process occurs in soils and sediments subjected to important drainage by meteoric water flows that take place in zones with a warm and humid climate [49]. In fact, these conditions could not be found in the studied area; therefore, kaolinite should have been inherited in the studied soils.

The simultaneous presence of kaolinite and palygorskite in appreciable quantities suggests that these minerals have undergone several processes. Indeed, the conditions of the genesis of these two clays are completely different. It is assumed that the genesis of these two clays did not take place at the same time [27].

Palygorskite is a common fibrous clay mineral in soils and sediments of arid and semiarid areas [50]. Many researchers have shown that the particular alkaline medium constituted by gypsum [34, 44] and calcite [64, 46] is favorable to neoformation of palygorskite. The high pH and activities of Si and Mg in the soil solution are the best conditions for palygorskite precipitation [37], especially in Neogene sediments [39, 40]. Although both calcareous and gypsiferous soils can provide buffered alkaline media with neces-

sary anions and cations for palygorskite crystallization, the characteristics of the solution chemistry of the gypsiferous soils may result in a more favorable medium for this purpose [7]. This hypothesis supports the positive correlation between palygorskite occurrence and gypsum/carbonate content in Oued Righ soils. According to the mineralogical data obtained by XRD shown in Table 2 and Table 1 for pedons 3, 5, 6, 7, and 13, these pedons are rich in calcite and gypsum and are the richest in palygorskite.

Various micromorphological studies were carried out on the soils of the northeastern Sahara desert of Algeria and showed that mineral clay occurs as coatings around detrital quartz skeleton grains (Fig. 6a) [19, 30, 75]. Scanning electron microscopic observation of clay coating on sand grains revealed a characteristic fibrous clay mineral, and electron microprobe analysis of clay plasma with a fibrous structure of certain gypsic horizons showed peaks of Si, Mg, and Al [28]. It is suggested that palygorskite is detrital in these soils, largely inherited from Mio-Pliocene parent material. According to an XRD analysis, Chellat et al. [15] noted that palygorskite is the dominant clay mineral in Mio-Pliocene rocks with a rate from 30 to 65%.

Palygorskite would have been formed in the Sahara during wetter periods than at present, preferably during the drying phase [24]. Therefore, its formation under hyperarid conditions is excluded. This mineral is stable in areas with precipitation levels less than 300 mm [63], and the conditions of its stability have not changed too much over time, which has allowed its preservation in the Sahara soil.

Furthermore, the nature of the clay assemblage in deep horizons of the analyzed pedons is similar, which suggests its heritage from parent rocks [53]. However, according to Boumaraf [11], one should be aware of the difference between the upstream and downstream Oued Righ. The upper Oued Righ with the current Saharan climatic context and a significant precipitation deficit does not offer favorable conditions for a possible reorganization of the silicate minerals initially degraded. Wind is the only particle mobilizing agent capable of creating a spatial distribution of secondary minerals beyond the limits of the lower Sahara. Downstream, the seasonal fluctuations in groundwater level allow silicate minerals (e.g., illite and chlorite) to find environments rich in basic ions that provide conditions for conservation or even transformation through the degradation of their crystalline systems.

Micromorphology study. The micromorphological properties of thin sections from selected soils varied vertically and laterally in the sampled pedons, with varying degrees of microstructure development and micropedological features. Table 3 briefly describes some micromorphological properties of selected soils. The overall microstructure of the studied soils ranged between massive, subangular blocky, spongy, and compact grains. The voids observed were commonly chambers and channels. The absence of porosity in certain thin sections indicates a very closed system in keeping with stronger cementation observed in the field, such as in pedons 1, 3 and 4. The coarse fraction consists mainly of subrounded to rounded quartz grains, feldspar, and fragments of limestone and gypsum. The roundness of the quartz grains increases with depth. The feldspar grains are generally smaller than the quartz grains and more subrounded in some pedons (1 and 4). Generally, coarse material is predominant in the most surface horizons. In contrast, in the deepest cemented horizons, there is a decrease in those coarse materials and porosity as a function of the increase in fine material.

Soil materials with fine fractions were usually red-brown; soils of this color (pedons 1, 4, 7 and 13) (Table 3) were dominated by illite and kaolinite [52]. The fine material of soil studies was silty-clayey to sometimes clayey, and brown–gray groundmass dominated in the soils with gypsiferous parent material (particularly pedons 2, 4, 5 and 10), whereas yellowish brown to bright brown groundmass prevailed in the soils with calcareous parent materials. Since soils are highly gypsiferous or calcareous, the b-fabric is mostly crystallitic. The coarse/fine material ratio (c/f) ranges from 2/8 in the pedon 2 horizon Bt to 8/2 in the pedon 1 horizon Bky, varying between chitonic and porphyric.

Moreover, the major pedofeatures were textural clay coatings (Figs. 6a and 6h) and infillings (Figs. 6b, 6g), crystalline aggregations, microcrystalline calcite, coatings on grains and infilling voids (Fig. 6e), calcite nodules (Figs. 6f, and 6h), microfossils (Fig. 6g), and gypsum crystals (Figs. 6a, 6b, 6c, 6d). The appearance of various types of pedofeatures within the studied soils, which were usually superimposed, is due to successive phases of pedogenesis under different pedoclimatic conditions. Subsequent weathering episodes are characterized according to the distribution of pedofeatures and their relative positions [45]. Different pedological processes are evident, and the chronological steps of their formation can be determined. The oldest phase is characterized by the growth of ferruginous nodules; a second phase is represented by clay illuviation; and the third phase is marked by strong calcite redistribution, fragmentation, and displacement of the clay coatings [76].

Calcite pedofeatures. Micromorphological observation showed three main primary types of calcitic features:

(1) Calcitic features of biogenic origin (microfossil) (Fig. 6g).

(2) Sparitic to micritic crystallizations of nodules of various sizes (Figs. 6e, 6g, 6h).

(3) Allochthonous sediment fragments with sharp boundaries (Fig. 6f).

Various calcitic pedofeatures confirm certain environmental conditions, including dissolution, migra-

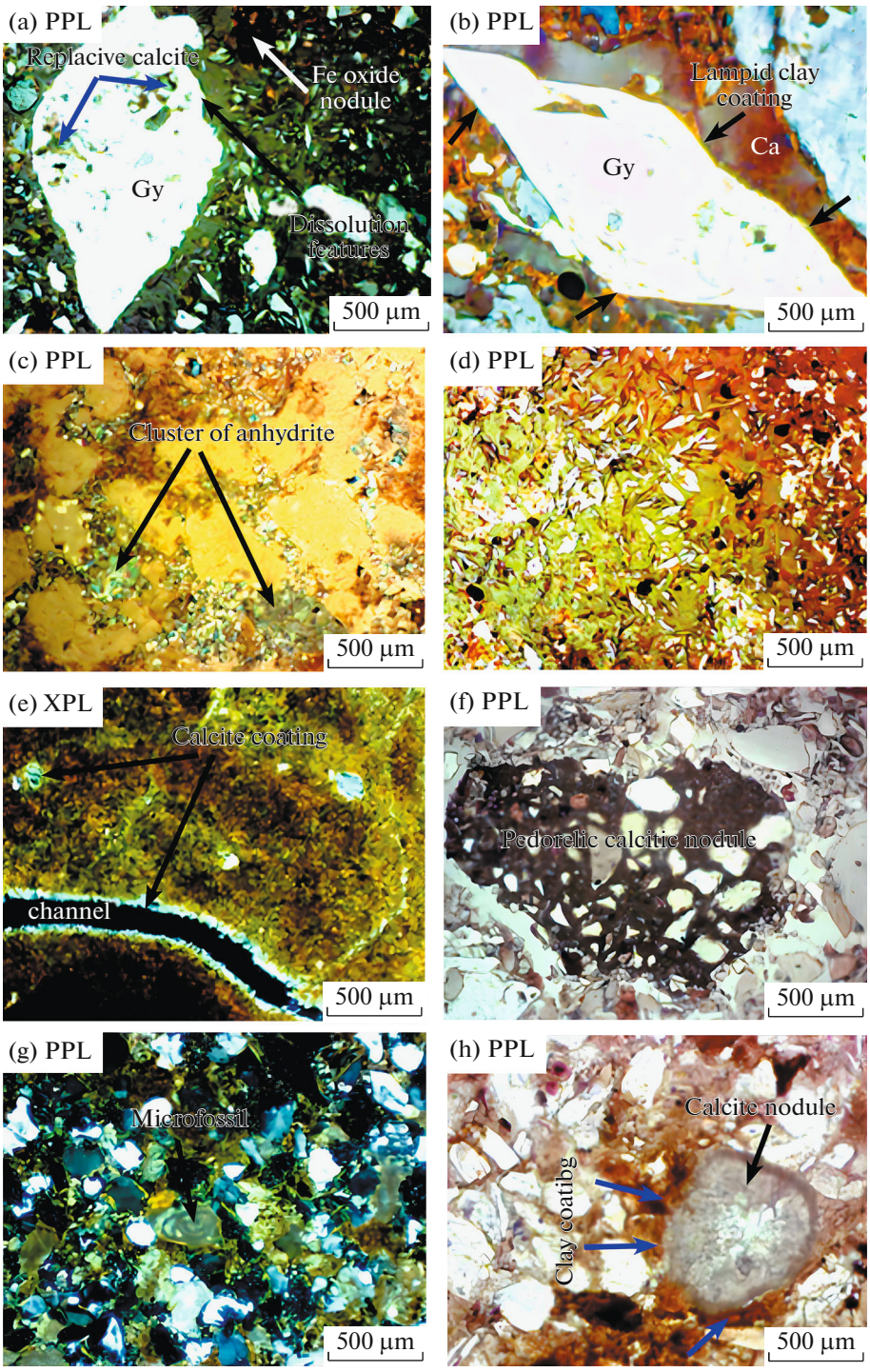

Fig. 6. Photomicrographs of crystalline pedofeatures in the studied soils (PPL—plane polarised light, XPL—crossed polarisers): (a) Ganular and lenticular gypsum crystals; large lenticular gypsum crystals (Gy) enrichied in calcite (blue arrow) and sand impurities from the matrix surrounded, with dissolution features (black arrow), the white arrow also shows nodule iron oxides in a groundmass, 1/Cky1; (b) Fin detrital material coating (black arrow) with dense calcitic (Ca) infilling cemented lenticular gypsum crystal (Gy), 4/2Cy; (c) Cluster anhydrite, 3/Bky; (d) fragmented micro–assembly of micro–crystalline gypsum and lenticular crystals, mixed with fine detritic material, 10/Cy1; (e) Calcitic coating in voids, 2/Btk; (f) pedorelic calcitic nodule embedded in detrial groundmass, 5/Cky1; (g) fossiloferous calcite, 7/C2; (h) Calcite nodule with clay coating, 13/Ckc1.

Table 3. Thin section description of the selected horizons studied

Pedon N/Hz	Microstructure	c/f ratio	b-fabric, color	Pedofeatures
1/Cky1	Weak developed massive, porosity (~5%)	5/5 porphyric	Crystallitic b-fabric, light brown	Many medium to large lenticular gypsum crystals, moderately with dissolution features and poikilitic calcite crystals inclusions. Few reddish Fe oxide nodules distributed in soil matrix
2/Btk	Weak to moderately developed subangular blocky (~15%)	2/8 Enaulic	Calcitic crystallitic, light grey to brown	Dense calcite infilling in voids and channels. Coating of sparitic calcite, along a horizotal fissure showing porostriation, dark reddish to black Fe/Mn oxides impregnation in matrix
3/Bky	Spongy structure, porosity (~5%)	4/6 porphyric	Gypsitic/Anhydritic crystallitic, light brown	Vermiform gypsum, Cluster of anhydrite in a brownish fine material with a strong brown accumulation of clay material.
4 /2Cy	Weak developed subangular blocky with porosity (~15%)	7/3 Porphyric	Gypsitic/calcitic crystallitic mostly and granostriated b-fabric, light grey to reddish yellow	Reddish yellow fine clay coatings around isolated coarse lenticular gypsum crystals (~0.8 mm in diameter), with infilling of calcite crystals
5/Cky1	Compact grain structure, porosity (~25%)	5/5 Chitonic-Porphyric	Calcitic crystallic b-fabric Light grey	Reworked sub-rounded calcitic nodules embedded in detrital sand grains groundmass
7/C2	Lntergrain microaggregate structure, porosity (~15%)	8/2 Chitonic-Porphyric	Grey Calcitic crystallic b-fabric yellowish brown	Loose calcite and clay infilling in voids, presence of a microfossil of the Miliolidae family with calcite nature
10/Cy1	Weak developed subangular, (45%)	7/3 Enaulic	Crystallitic b-fabric, light brown	Loose continuous infilling composed of lenticular and sub-lenticulare gypsum crystal
13/Ckc	Compact grain, porosity (~25%)	6/4 Porphyric	Calcitic crystallic b-fabric Light brown	Rounded calcitic nodules with clay coating with Fe oxides (~5%) in ground mass

tion, and sedimentation processes that existed during their formation [64]. According to Khormali et al. [42], the type and morphology of calcitic pedofeatures are mainly characterized by soil moisture and temperature regimes.

The carbonate character was established by the predominance of porphyric-related distribution (pedons 2, 5, 7, and 13) and crystallitic b-fabric in the groundmass. The lower content of calcitic nodules (various sizes) was mostly randomly distributed on detrital sand grain groundmass in the more arid areas, which could be explained by lower precipitation slowing down the process of dissolution–recrystallization and therefore limiting the formation of nodules [41].

The morphology of the orthic calcite nodules (Figs. 6g, 6h) and their arrangement in the groundmass suggest that they were formed by dissolution/recrystallization in situ. The size of the nodules increased with the increase in the concentrated calcite crystals. Relic calcitic nodules (Fig. 6f) commonly have more similar internal microfabric than the calcarous bedrocks and calcic horizons of upstream soils. The rounded shape of nodules reflects their transportation and redeposition by floodwaters. During the wet phases, the action of water at low pCO_2 dissolves part of the carbonates of the calcareous crust, the dispersion of the fragments of calcrete favored the displacement of these fine grains by the wind during the

arid phase, and the alternation of phases of aeolian and water erosion caused the burial of pedorelics in the detrital sandy material.

Conversely, recrystallization of illuviated calcium carbonate from surface horizons caused the formation of calcite coatings (Fig. 6e). The limpid color of the coatings proved that no impurities were associated with calcium carbonate and that the coatings were formed during arid periods [21]. Calcite infillings seem to be formed when soluble pedogenic carbonate crystals progressively fill the pore space between the grains in the arid conditions of the area (Fig. 6g).

Furthermore, carbonate masses and clay coatings were observed in argillic and calcic horizons (Figs. 6g, 6h). The current arid climate does not have enough humidity to form these horizons [62], and clay translocation occurred during more humid periods, and was deposited during dryer periods. The repeated cycles of wetting and drying caused the formation of the abovementioned morphological features on a stable surface. The presence of carbonates in Oued Righ soils indicated a more humid paleoclimate in the history of the area; the micromorphological observations support these findings. The processes of accretion of calcite were discontinuous at geological time scale. Discontinuities result from the variations in water table depth, the intensity of evaporation, soil water composition, and the intensity of calcitic dust aggradation [25].

Gypsum pedofeatures. The micromorphological observations have investigated the gypsum in pedon1 (tabular butte), pedon 3 (alluvial plain), pedon 4 (clay quarry), and pedon 10 (piedmont). Gypsum occurrence in soils of the study area revealed that local environmental conditions with low rainfall prohibited he leaching of this mineral. The different forms of gypsum crystals in the studied soils are related to microenvironmental changes during soil formation [30].

Lenticular (Figs. 6a, 6b, 6d), granular (Fig. 6d), and vermiform (Fig. 6c) crystals are the dominant pedofeatures observed in the thin sections of pedons 1/Cky1, 4/2Cy, 3/Bky1, and 10/Cy1 (Figs. 6a, 6b, 6d). Lenticular gypsum represents the most common morphology of gypsum in soils and has been described by many authors [34, 56, 57]. The lenticular gypsum has no preferred orientation and was found in the soil matrix and inside voids. Lenticular gypsum crystals can be formed under any environmental condition [38]. However, Amit and Yaalon [2] cited two major processes proposed for crystallization of lenticular gypsum: ion impurities within the soil solution or crystallization in a void system where space is not limiting.

Poch et al. [56] proved that massive crusts or subsurface petrogypsic horizons were characterized by large lenticular crystals (1/Cky1 and 4/2Cy, Figs. 6a and 6b), the formation of which presumably took a very long time. Our results indicate that lenticular gypsum crystals were more abundant in subsurface horizons than in the surface ones. Jafarzadeh and Burnham [38] reported similar facts in arid regions of Iran.

Most of the macro gypsum crystals form inclusive or incorporative fabrics (poikilotopic crystals) that contain impurities with the same size and composition as those of the surrounding matrix materials (Figs. 6a, 6b). The impurities are calcite and quartz crystals, scattered randomly. Crusts are occasionally made up of lenticular crystals greater than 1 mm in diameter. In those exhibiting porphyroblastic gypsum crystals, quartz grains may be included poikilitically within the crystals [73].

The relative abundance of pseudomorphoses of lenticular gypsum in calcite inside the microsparitic micromass characterizes the gypsum-saline soils of arid areas such as the upper Oued Righ region (pedon 1 and pedon 4). Hamdi-Aissa [31] and Poch et al. [56] considered them indicators of a more arid climate in the past, followed by more humid conditions. One additional feature observable in some calcite-rich matrices is a decalcification process accompanying gypsum formation. The zone around the pockets of the gypsum may be decalcified, so calcite supplied calcium for the gypsum.

Sullivan [69] proposed two mechanisms for pseudomorph formation in soil: gypsum dissolution proceeded by calcite precipitation in the void pseudomorph, and the second is the replacement of gypsum by calcite. The former could explain pseudomorphs in the groundmass, with voids functioning as molds but not loose infillings in pores. The second mechanism is supported by the occurrence of partially replaced crystals, which was the case observed in the studied samples (Figs. 6a, 6b) [68].

Corroded gypsum crystals were common in the subsurface horizons of pedons 1, 4, and 10. Corrosion of some gypsum crystals was observed along one side of lenticular crystals and in the other crystals observed along all margins of undefined gypsum crystals (Figs. 6a, 6b, 6d). The corroded gypsum crystals have slightly to highly embayed and engulfed margins filled with clay and carbonates. The depth and morphology of the embayed and engulfed margins of corroded gypsum vary according to the intensity of corrosion among adjacent crystals [4].

Anhydrite occurs near the soil surface in arid regions and is mainly formed by total dehydration of gypsum due to higher temperatures. Hence, micromorphological observations in the present research revealed the formation and growth of anhydrite crystals after the vermiform of gypsum in a fine brownish material.

The appearance of randomly oriented and distributed anhydrite crystals inside gypsum crystals could be attributed to the dehydration process [5]. The replacement of gypsum crystals with bassanite or anhydrite can result in perfectly pseudomorphic aggregate for-

mation [47]. Anhydrite occurred as pseudomorphs of gypsum crystals in pedon 3 horizon Byk (Fig. 6c).

Compound pedofeatures were found in pedons 4 and 13 (Figs. 6b, 6h). These pedofeatures characterized the temporal sequence of soil formation processes and paleoenvironmental conditions. The formation of this juxtaposed compound pedofeature is ascribed to the variation in local environmental conditions. The coating of calcite nodules and gypsum crystals on clay particles was caused by the more humid climate followed by an arid period, which formed a polygenetic soil.

CONCLUSIONS

Different soils of the Oued Righ region were studied on various landscape units and geological strata using a multianalytical technique. The physicochemical, mineralogical, and micromorphological characteristics of the studied soils were closely influenced by landscape position, parent material and paleoenvironment conditions. The soils of the study area were generally alkaline with high proportions of gypsum in different accumulation forms, highly saline, poor in organic matter, and aerated on the surface. More developed soils were found on the stable plateau and piedmont plain. The appearance of calcic-gypsic horizons in the studied pedons was induced by the spatial distribution of calcareous and gypsiferous geological strata. The textural heterogeneity observed in the deep horizons was caused by successive phases of erosion and filling of the valley bottom, as opposed to the upper horizons, which have an aeolian origin. The hyperarid climate of the Oued Righ region favors the concentration and crystallization of salts in the soil, both on the surface and in depth, depending on environmental conditions. The soils become hydromorphic in poorly drained sites composed of fine alluvia such as salt depressions and ancient palm groves located at the bottom of the Oued Righ valley. The studied soils were classified as Aridisols (Petrogypsids, Haplogypsids, Calcigypsids, and Argigypsids) and Entisols (Torrifluvents, Torripsamments) in Soil Taxonomy (2014). They were classified as Gypsisols, Arenosols, Fluvisols and Solonchaks in the WRB (2022). Although the present environmental conditions, climate, and parent material are very appropriate for the production of Gypsisols or Haplogypsids, the role of two other factors, i.e., time and topography, restrict their development to only favorable positions. The clay minerals identified in almost all landscape surfaces were palygorskite, kaolinite, chlorite-smectite and illite with more palygorskite and less smectite in the soils with gypsiferous parent materials. The clay mineralogy results indicated that inheritance might be the primary source of these minerals. Micromorphological observations clearly showed soil records of different climatic conditions in the history of the Oued Righ region; clay coatings and infillings, calcite coatings on grains and voids, calcite nodules, gypsum crystals and Fe and Mn oxide nodules were common pedofeatures observed in the thin sections of the studied soils; probably they were formed in a former climate with more available moisture. More research in this region and similar regions of the Algerian Sahara is strongly encouraged to confirm and deepen the findings presented in this study.

ACKNOWLEDGMENTS

We thank the Laboratory of Biogeochemistry of Desert Areas and the Agronomy Department of Ouargla University (Algeria), the Laboratory of CRSTRA for providing the work environment, and INRAE-AgroPariTech, Paris-Grignon, France for manufacturing soil thin sections. The authors would like to thank Mr. Halis youcef for his valuable help.

FUNDING

This work was supported by the Directorate General of Scientific Research and Technological Development, Algeria (DGRSDT) through the Val-Ped-Oasis project (Valorisation des données pédologiques des oasis du Bas Sahara) (grant number FNRSDT-2017).

CONFLICTS OF INTEREST

The authors declare no conflict of interest.

AUTHOR CONTRIBUTIONS

All authors have read and agreed to the published version of the manuscript.

REFERENCES

1. H. Abbaslou and A. Abtahi, "Origin and distribution of clay minerals in calcareous, gypsiferous, saline soils and sediments of Bakhtegan Lake bank, Southern Iran," Iran Agric. Res. **25** (2), (2007). https://doi.org/10.22099/IAR.2008.187
2. R. Amit and D. H. Yaalon, "The micromorphology of gypsum and halite in Reg soils - The Negev desert, Israel," Earth Surf. Processes Landforms **21** (12), 1127–1143 (1996). https://doi.org/10.1002/(sici)1096-9837(199612)21:12<1127::aid-esp656>3.0.co;2-g
3. P. Anne, "Sur le dosage rapide du carbone organique des sols," Ann. Agron. **2** (1), 161–172 (1945).
4. M. A. Aref and A. A. Mannaa, "The significance of gypsum morphology in interpreting environmental changes caused by human construction, Red Sea coastal evaporation environment, Saudi Arabia," Environ. Earth Sci. **80** (2), 1–21 (2021). https://doi.org/10.1007/s12665-020-09298-4
5. M. A. M. Aref, "Classification and depositional environments of Quaternary pedogenic gypsum crusts (gypcrete) from east of the Fayum depression, Egypt,"

Sediment. Geol. **155** (1–2), 87–108 (2003). https://doi.org/10.1016/s0037-0738(02)00162-8

6. G. Aubert, *Methodes d'analyses Des Sols: Documents de Travail Tous Droits Reserves* (Centre régional de documentation pédagogique, 1978).
7. P. Azizi, S. Mahmoodi, and H. Torabi, "Morphological, physico-chemical and clay mineralogy investigation on gypsiferous soils in southern of Tehran, Iran," Middle-East J. Sci. Res. **7** (2), 153–161 (2011).
8. J. L. Ballais, "Des oueds mythiques aux rivières artificielles: l'hydrographie du Bas-Sahara algérien," Physio-Géo. Géogr. Phys. Environ. **4**, 107–127 (2010).
9. M. Benchetrit, "Les sols d'Algérie," Rev. Géogr. Alp. **44** (4), 749–761 (1956).
10. BNEDER, *Agro-Pedological Study in the Region of Ouargla, Study Report* (1992).
11. B. Boumaraf, *Caractéristiques et Fonctionnement des Sols Dans la Vallée de Oued Righ, Sahara Nord Oriental Algérie* (2013). http://www.theses.fr.
12. T. G. Boyadgiev, *Contribution to the Knowledge of Gypsiferous Soils* (FAO, Rome, 1974).
13. P. Bullock, N. Fedoroff, A. Jongerius, G. Stoops, T. Tursina, and others, *Handbook for Soil Thin Section Description* (Waine Research, 1985).
14. O. A. Chadwick, J. M. Sowers, and R. G. Amundson, "Morphology of calcite crystals in clast coatings from four soils in the Mojave Desert region," Soil Sci. Soc. Am. J. **53** (1), 211–219 (1989). https://doi.org/10.2136/sssaj1989.03615995
15. S. Chellat, S. Bourefis, and H. A. Belhadj, "Paleoenvironemental reconstitution of mio- pliocenes sandstones of the lower-Sahara at the base of exoscopic and sequential analysis," La Pensee **76** (7), 34–51 (2014).
16. X. Y. Chen, "Pedogenic gypcrete formation in arid central Australia," Geoderma **77** (1), 39–61 (1997). https://doi.org/10.1016/s0016-7061(97)00005-0
17. R. U. Cooke, A. Warren, and A. S. Goudie, *Desert Geomorphology* (CRC Press, 1993). https://doi.org/10.1016/0013-7952(93)90027-a
18. Coutinet, *Méthodes d'Analyses Utilisables Pour Les Sols Salés, Calcaires et Gypseux. Analyses D'eaux* (1965).
19. B. Djili and B. Hamdi-Aïssa, "Characteristics and mineralogy of desert alluvial soils: Wadi Zegrir, Northern Sahara of Algeria," Arid Land Res. Manage. **32** (1), 1–19 (2018). https://doi.org/10.1080/15324982.2017.13844
20. J. H. Durand and J. Guyot, *L'irrigation des Cultures Dans l'Oued Righ* (1955).
21. N. Durand, H. C. Monger, and M. G. Canti, *Calcium Carbonate Features. U: Stoops G, Marcelino V, Mees F (ur.) Interpretation of Micromorphological Features of Soils and Regoliths* (2010).
22. P. A. Dutil, *Contribution à l'étude Des Sols et Des Paléosols Du Sahara* (1971).
23. N. Fedoroff and M. A. Courty, "Organisation du sol aux échelles microscopiques," Pédologie **2**, 349–375 (1994).
24. N. Fedoroff and M. Courty, "Indicateurs pedologiques d'aridification; exemples du Sahara," Bull. Soc. Geol. Fr. **1**, 43–53 (1989). https://doi.org/10.2113/gssgfbull.v.1.43
25. N. Fedoroff, M. A. Courty, and Z. Guo, *Palaeosoils and Relict Soils* (2010). https://doi.org/10.1016/B978-0-444-53156-8.00027-1
26. P. Guilloré, *Méthode de Fabrication Mécanique et en Série des Lames Minces*, 3éme éd (Ina Paris-Grignon, 1985).
27. A. Halitim, *Sols Des Régions Arides d'algerie* (Office des Publications Universitaires, 1988).
28. B. Hamdi Aissa and N. Fedoroff, "Macro and micromorphology of gypsum in desertic soils (Northern Sahara. Algéria)," in *Proceeding of the International Symposium on Soils with Gypsum. Lleida, Catalonia, Spain* (1996).
29. B. Hamdi-Aissa and M.-C. Girard, "Utilisation de la télédétection en régions sahariennes, pour l'analyse et l'extrapolation spatiale des pédopaysages," Science et Changements Planétaires/Sécheresse **11** (3), 179–188 (2000).
30. B. Hamdi-Aïssa, *Le Fonctionnement Actuel et Passé de Sols du Nord Sahara (Cuvette de Ouargla). Approches Micromorphologique, Géochimique, Minéralogique et Variabilité Spatiale* (2001).
31. B. Hamdi-Aissa, "Paleogeochemical interpretation of some gypsic microfabrics in hyper-desert soils," in *ISSS Ed, 17th World Congress of Soil Science, Bangkok* (2002), pp. 1–9.
32. B. Hamdi-Aissa, V. Valles, A. Aventurier, and O. Ribolzi, "Soils and brine geochemistry and mineralogy of hyperarid desert playa, Ouargla basin, Algerian Sahara," Arid Land Res. Manage. **18** (2), 103–126 (2004). https://doi.org/10.1080/15324804902796560
33. A. Hammadi, A. Brinis, and N. Djidel, "Hydrodynamic characteristics of the "Complex Terminal" aquifer in the region of Oued Righ North (Algerian Sahara)," **9**, 3075–3081 (2023).
34. S. S. Hashemi, M. Baghernejad, and H. Khademi, "Ar ch ive ive," **13**, 273–288 (2011).
35. J. Herrero, O. Artieda, and D. C. Weindorf, "The determination of gypsum in soils," Soil Sci. Soc. Am. J. **82** (2), 293–294 (2018). https://doi.org/10.2136/sssaj2017.12.0429
36. S. Hillier, *DM Moore \& RC Reynolds Jr. X-ray Diffraction and the Identification and Analysis of Clay Minerals* (Oxford University Press, 1997). xvii+ 378 pp. Price£27.95 ISBN: 0-19-508713-5.," clay Miner. **34**(1), 210–211 (1999).
37. S. Hojati and H. Khademi, *Genesis and Distribution of Palygorskite in Iranian Soils and Sediments*, 1st ed. (Elsevier B.V., 2011), vol. 3. https://doi.org/10.1016/B978-0-444-53607-5.00008-6
38. A. Jafarzadeh and C. P. Burnham, "Gypsum crystals in soils," J. Soil Sci. **43** (3), 409–420 (1992). https://doi.org/10.1111/j.1365-2389.1992.tb00147.x

39. H. Khademi and A. R. Mermut, "Source of palygorskite in gypsiferous Aridisols and associated sediments from central Iran," Clay Miner. **33** (4), 561–578 (1998). https://doi.org/10.1180/000985598545895

40. F. Khormali and A. Abtahi, "Origin and distribution of clay minerals in calcareous arid and semi-arid soils of Fars Province, southern Iran," Clay Miner. **38** (4), 511–527 (2003). https://doi.org/10.1180/0009855023740112

41. F. Khormali, A. Abtahi, and G. Stoops, "Micromorphology of calcitic features in highly calcareous soils of Fars Province, Southern Iran," Geoderma **132** (1–2), 31–46 (2006). https://doi.org/10.1016/j.geoderma.2005.04

42. F. Khormali, A. Abtahi, S. Mahmoodi, and G. Stoops, "Argillic horizon development in calcareous soils of arid and semiarid regions of southern Iran," Catena **53** (3), 273–301 (2003). https://doi.org/10.1016/s0341-8162(03)00040-7

43. N. Koull, M. Kherraze, K. Lakhdari, T. Benzaoui, S. Helimi, M. S. Laouissat, Y. Kherfi, A. Bougafla, and M. T. Benazzouz, "Eaux d'irrigation et salinisation des sols des perimetres irrigues dans la vallee de L' Oued Righ," J. Algérien des Régions Arides, 97–102 (2013).

44. J. B. Kowalska, M. Skiba, K. Maj-szeliga, R. Mazurek, and T. Zaleski, "Does calcium carbonate influence clay mineral transformation in soils developed from slope deposits in Southern Poland?," J. Soils Sediments **21**, 257–280 (2021). https://doi.org/10.1007/s11368-020-02764-3.

45. P. Kühn, J. Aguilar, R. Miedema, and M. Bronnikova, "Textural pedofeatures and related horizons," in *Interpretation of Micromorphological Features of Soils and Regoliths* (Elsevier, 2018), pp. 377–423. https://doi.org/10.1016/B978-0-444-63522-8.00014-0

46. A. Lopez-Galindo, A. Ben Aboud, P. F. Hach-Ali, and J. C. Ruiz, "Mineralogical and geochemical characterization of palygorskite from Gabasa (NE Spain). Evidence of a detrital precursor," Clay Miner. **31** (1), 33–44 (1996).

47. F. Mees and T. V Tursina, *Chapter 11 Salt Minerals in Saline Soils and Salt Crusts* (Elsevier B.V., 2018). https://doi.org/10.1016/B978-0-444-63522-8.00011-5

48. M. Morris, R. Cervigni, Z. Guo, and J. Koo, "The Central Role of Drylands in Africa's Development Challenge," in *Confronting Drought Africa's Drylands Oppor. Enhancing Resil.* (2016), pp. 27–36.

49. M. Nadimi and M. H. Farpoor, "Genesis and clay mineralogy of soils on different geomorphic surfaces in Mahan-Joupar area, central Iran," Arabian J. Geosci. **6** (3), 825–833 (2013). https://doi.org/10.1007/s12517-011-0350-3

50. A. Neaman and A. Singer, "The effects of palygorskite on chemical and physico-chemical properties of soils: a review," Geoderma **123** (3–4), 297–303 (2004). https://doi.org/10.1016/j.geoderma.2004.02

51. W. D. Nettleton and Soil Science Society of America, *Occurrence, Characteristics, and Genesis of Carbonate, Gypsum, and Silica Accumulations in Soils* (1991). https://doi.org/10.1097/00010694-199306000-00010

52. K. Norrish and J. G. Pickering, *Clay Minerals in Soils: an Australian Viewpoint* (CSIRO, Acad. Press, 1983), vol. **281**, p. 308.

53. F. E. Omdi, L. Daoudi, and N. Fagel, "Origin and distribution of clay minerals of soils in semi-arid zones: example of Ksob watershed (Western High Atlas, Morocco)," Appl. Clay Sci. **163**, 81–91 (2018). https://doi.org/10.1016/j.clay.2018.07.013

54. ONM, *Données Climatiques de La Région de l'Oued Righ. Algeria: Report of the National Office of Meteorology, Touggourt* (2017).

55. H. Owliaie, M. N. Ghiri, and S. Shakeri, "Soil-landscape relationship as indicated by pedogenesis data on selected soils from Southwestern, Iran," Eurasian J. Soil Sci. **7** (2), 167–180 (2018). https://doi.org/10.18393/ejss.376284

56. R. M. Poch, O. Artieda, and M. Lebedeva, "Gypsic features," in *Interpretation of Micromorphological Features of Soils and Regoliths* (2018), pp. 259–287.

57. R. M. Poch, W. De Coster, and G. Stoops, "Pore space characteristics as indicators of soil behaviour in gypsiferous soils," Geoderma **87** (1–2), 87–109 (1998). https://doi.org/10.1016/s0016-7061(98)00068-8

58. M. Pouget, "Contribution à l'étude des croûtes et encroûtements gypseux de nappe dans le sud Tunisien," Cah ORSTOM, Ser. Pedofil **6** (3), (1968).

59. H. L. Richard and L. S. Donald, "Carbonate and gypsum," Methods Soil Anal. **3**, 437–474 (1996).

60. M. Robert and D. Tessier, *Méthode de Préparation des Argiles des Sols Pour des Etudes Minéralogiques* (1974).

61. F. J. Sangüesa, J. Arostegui, and I. Suarez-Ruiz, "Distribution and origin of clay minerals in the Lower Cretaceous of the Alava Block (Basque-Cantabrian Basin, Spain)," Clay Miner. **35** (2), 393–410 (2000). https://doi.org/10.1180/000985500546864

62. M. Sarmast, M. H. Farpoor, A. Jafari, and I. E. Borujeni, "Tracing environmental changes and paleoclimate using the micromorphology of soils and desert varnish in central Iran," Desert **2**, 331–353 (2019). https://doi.org/10.22059/JDESERT.2019.76389

63. A. Singer, "Palygorskite and sepiolite group minerals," Miner. Soil Environ. **1**, 829–872 (1989). https://doi.org/10.2136/sssabookser1.2ed.c17

64. A. Singer, W. Kirsten, and C. Bühmann, "Fibrous clay minerals in the soils of Namaqualand, South Africa: characteristics and formation," Geoderma **66** (1–2), 43–70 (1995). https://doi.org/10.1016/0016-7061(94)00052-c

65. SOGREAH, *Participation in the Development of the Oued Righ. Agropedological Study* (1970).

66. S. S. Soil, "Keys to soil taxonomy," Soil Conserv. Serv. **12**, 410 (2014).

67. G. Stoops, "Micromorphology as a tool in soil and regolith studies," in *Interpretation of Micromorphological Features of Soils and Regoliths* (2018), pp. 1–19. https://doi.org/10.1016/b978-0-444-53156-8.00001-5

68. G. Stoops, *Guidelines for Analysis and Description of Soil and Regolith Thin Sections* (John Wiley \& Sons, 2021), vol. 184.

69. L. A. Sullivan, "Micromorphology and genesis of some calcite pseudomorphs after lenticular gypsum," Aust. J. Soil Res. **28** (4), 483–485 (1990). https://doi.org/10.1071/sr9900483

70. M. Thiry, "Palaeoclimatic interpretation of clay minerals in marine deposits: an outlook from the continental origin," Earth-Sci. Rev. **49** (1–4), 201–221 (2000). https://doi.org/10.1016/s0012-8252(99)00054-9

71. P. Verrecchia and L. Trombino, "Observation of soils: from the field to the microscope," in *A Visual Atlas for Soil Micromorphologists* (2021), pp. 1–17. https://doi.org/10.1007/978 -3-030-67806-7

72. K. Vos, N. Vandenberghe, and J. Elsen, "Surface textural analysis of quartz grains by scanning electron microscopy (SEM): from sample preparation to environmental interpretation," Earth-Sci. Rev. **128**, 93–104 (2014). https://doi.org/10.1016/j.earscirev.2013.10.013

73. A. Watson, "Desert gypsum crusts as palaeoenvironmental indicators: a micropetrographic study of crusts from southern Tunisia and the central Namib Desert," J. Arid Environ. **15** (1), 19–42 (1988). https://doi.org/10.1016/S0140-1963(18)31002-4

74. *WRB. World Reference Base for Soil Resources. International Soil Classification System for Naming Soils and Creating Legends for Soil Maps*, 4th ed. (International Union of Soil Sciences (IUSS), Vienna, 2022).

75. F. Youcef and B. Hamdi-Aïssa, "Paleoenvironmental reconstruction from palaeolake sediments in the area of Ouargla (Northern Sahara of Algeria)," Arid Land Res. Manage. **28** (2), 129–146 (2014). https://doi.org/10.1080/15324982.2013.84130

76. F. Zahi, A. Drouichee, N. Bouchahm, W. Hamzaoui, W. Chaib, and L. Djabri, "The water upwelling in Oued Righ valley: inventory and caracterization," J. Mater. Environ. Sci. **2** (SUPPL. 1), 445–450 (2011).

77. A. Zerboni, L. Trombino, and M. Cremaschi, "Micromorphological approach to polycyclic pedogenesis on the Messak Settafet plateau (central Sahara): formative processes and palaeoenvironmental significance," Geomorphology **125** (2), 319–335 (2011). https://doi.org/10.1016/j.geomorph.2010.10

78. M. Zouidi, A. H. Borsali, A. Allam, and R. Gros, "Characterization of coniferous forest soils in the arid zone," For. Stud. **68** (1), 64–74 (2018). https://doi.org/10.2478/fsmu-2018-0006